Hemimandibular Hyperplasia Correction by Simultaneous Orthognathic Surgery and Condylectomy Under Digital Guidance

Bing Han, DDS, Xing Wang, MD, PhD,† Zili Li, DDS, MD,‡ Biao Yi, DDS, MD,§ Cheng Liang, DDS, MD,|| and Xiaoxia Wang, DDS, PhD¶*

Purpose: Orthognathic surgery with simultaneous condylectomy under digital guidance has been proved to be a feasible method to treat hemimandibular hyperplasia (HH). The objective of this study was to evaluate the effects and precision of correction of HH by use of this method.

Patients and Methods: This was a case-series study. Fourteen patients with HH who had undergone simultaneous bimaxillary orthognathic surgery and condylectomy from January 2016 to April 2017 were included in this study. Presurgical virtual treatment planning was performed, transferred to the operation room, and realized with the assistance of surgical navigation and 3-dimensionally printed occlusion splints. Postoperative computed tomography data were used to analyze improvement in facial symmetry and verify the accuracy of the surgical procedure.

Results: All patients exhibited satisfactory clinical effects; facial asymmetry was corrected as expected. Postoperative validation showed that the presurgical planning had been achieved more precisely on the unaffected side than on the affected side. Moreover, bilateral mandibular proximal segments showed a tendency for outward rotation compared with the presurgical planning model. Furthermore, when we assessed facial symmetry compared with the presurgical model, deviation of all midline landmarks was less than 2 mm, occlusal-plane inclination was less than 1 mm, and the asymmetry index of paired landmarks was remarkably decreased after surgery ($P < .01$).

Conclusions: Orthognathic surgery with simultaneous condylectomy under digital guidance is a realistic and precise method for treatment of HH. Surgical results can be validated during surgery by virtual navigation. However, movement of each bone segment cannot be accurately controlled as planned before surgery.

J Oral Maxillofac Surg 76:1563.e1-1563.e18, 2018

Hemimandibular hyperplasia (HH) is a developmental deformity, first reported by Adams[1] in 1836. It is a type of condylar hyperplasia, the other 2 types of which are hemimandibular elongation and hybrid forms of HH and hemimandibular elongation; this classification was put forward by Obwegeser and Makek[2] in 1986

Received from Department of Oral and Maxillofacial Surgery, Peking University School and Hospital of Stomatology, Beijing, China.

*Resident.

†Professor.

‡Professor and Department Head.

§Professor.

||Chief Physician.

¶Chief Physician and Associate Professor.

This study was supported by the Capital Characteristic Clinical Research Projects (Z161100000516114).

Conflict of Interest Disclosures: None of the authors have any relevant financial relationship(s) with a commercial interest.

Presented in part at the 23rd International Conference on Oral & Maxillofacial Surgery, April 2, 2017, Hong Kong, China.

Address correspondence and reprint requests to Dr Wang: 22 Zhongguancun South Avenue, Haidian District, Beijing 100081, China; e-mail: doctorwang66@sina.com

Received November 15 2017

Accepted March 9 2018

0278-2391/18/30219-2

https://doi.org/10.1016/j.joms.2018.03.006

and is used widely. HH is characterized by unilateral 3-dimensional (3D) enlargement of the mandible including the condyle, condylar neck, ascending ramus, and mandibular body, which usually terminates at the symphysis. This results in facial asymmetry and deformity, occlusal disorder and temporomandibular joint (TMJ) dysfunction, deviation of the midpoint of the chin to the unaffected side, bowing of the inferior alveolar nerve canal and inferior margin of the involved mandible, a tilted occlusal plane and malocclusion, and pain, as well as clicking and snapping in the TMJ, along with other mandibular mobility disorders. Treatment for each of these differs based on the diagnosis.[3] HH can be diagnosed through clinical, radiologic, bone scanning, and histologic manifestations.[2,4-6] Typically, orthognathic surgery with simultaneous condylectomy[7,8] can produce functional and esthetic results.[9-11]

Surgical approaches for condylectomy vary widely. Preauricular transcutaneous access is the most classic approach because it provides good visual access to the condyle, condylar neck, and glenoid fossa[12]; moreover, it can be combined with the submandibular approach, temporal extension, or zygomatic arch sectioning, if necessary.[13-15] Apart from the white population, scars after skin incisions can be distinctly seen in the Mongoloid population; thus, ethnicity should be particularly taken into account in patients who have a strong desire to avoid facial skin incisions. An intraoral approach for condylectomy was introduced to avoid unesthetic facial skin scars, facial nerve injury, and salivary fistulae.[16] By use of intraoral vertical ramus osteotomy, complete resection of any condylar lesion and favorable TMJ reconstruction can be achieved under direct vision. However, extensive dissection of the condyle and ramus as well as the free bone graft may lead to poor vascularity, bone resorption, and relapse of facial asymmetry.[17,18] Intraoral condylectomy via coronoid process resection was first reported in 2011.[16] A previous study emphasized exploring the feasibility of this surgical method and showed that it can be safely implemented with no remarkable complications.[19] Furthermore, surgical procedures assisted by endoscopic and surgical navigation can help achieve acceptable accuracy with minimal invasiveness.[16,17,20] However, owing to simultaneous mandibular sagittal split osteotomy (SSO) and condylectomy, it can be extremely difficult to precisely position the condylar stump into the glenoid fossa of the affected side.

We evaluated the precision of HH treatment via an intraoral approach that was assisted by 3D computer-aided design and computer-aided manufacturing (CAD-CAM) technologies as well as surgical navigation. Our study aimed to identify any shortcomings, disadvantages, or inadequacies of this novel technique, which would further guide us to improve the design as well as the surgical process and achieve better surgical outcomes in the future.

Patients and Methods

From January 2016 to April 2017, 14 patients who underwent simultaneous bimaxillary orthognathic surgery and intraoral condylectomy via coronoid process resection at the Department of Oral and Maxillofacial, Peking University School of Stomatology, were included in this study. The inclusion criteria were *1)* patients diagnosed with HH who required simultaneous bimaxillary orthognathic surgery, condylectomy, and mandibular inferior border contouring; *2)* condylectomy via coronoid process resection performed using an intraoral approach; *3)* use of 3D analysis and virtual treatment planning; *4)* application of surgical navigation; and *5)* adequate records for completion of analysis. The exclusion criteria were *1)* patients in whom the procedures outlined in the inclusion criteria were not indicated, *2)* patients who refused to proceed with the planned surgical procedures, and *3)* inadequate records.

The chief complaints of these patients were gradual facial asymmetry and disordered occlusion over the years. Before surgery, occlusal canting was noted in all patients, and occlusal disorders, including open bite or locked occlusion, on the affected side were noted in 11 patients. Preoperative orthodontic therapy was performed in 2 patients. According to technetium 99m (^{99m}Tc) bone scan, the uptake ratio between the affected and unaffected condyles ranged from 1.15 to 2.63. All patients provided written informed consent before participation. The study was approved by the institutional review board of Peking University School of Stomatology.

PREOPERATIVE CAD-CAM

After hospital admission, the history and physical examination details were recorded. Subsequently, a radiographic study was performed for diagnosis and presurgical planning. Scintigraphy using ^{99m}Tc indicated the necessity for condylectomy. The natural head position was recorded using the 3dMDface System (3dMD, Atlanta, GA) and the laser level method.[21,22] Computed tomography (CT) data of patients were processed using Super Virtual software (version 1.0; Byteking, Beijing, China) and used for 3D analysis and virtual treatment planning. Surgical navigation was planned using iPlan CMF (version 3.0; Brainlab, Munich, Germany). Intermediate and terminal occlusal splints were produced using CAD-CAM technology.

First, we determined the osteotomy line at the condylar head based on the extent of the bony lesion noted on spiral CT images, along with the difference in ramus height bilaterally (Fig 1). Subsequently, Le Fort I osteotomy and bilateral SSO (BSSO) were performed to correct the canted occlusion level as well as the mandible. Next, the proximal segment of the affected mandible was pushed upward into the glenoid fossa to reconstruct the TMJ structure. Thereafter, the inferior borders of both sides of the mandible were compared to ascertain whether mandibular contouring was needed to achieve facial symmetry; the range of resection of the inferior mandibular border was marked, if necessary (Fig 2). Finally, genioplasty was performed to further improve facial symmetry. Intermediate occlusal splints were determined using the postoperative maxilla and the preoperative mandible. Terminal occlusal splints were determined based on the final occlusion; these were designed by engineers, fabricated using biocompatible materials (Med-610; Stratasys, Rehovot, Israel), and manufactured through 3D printing by means of a Stratasys Objet30 3D printer (Fig 3).

After virtual treatment planning, the files for surgical navigation were compiled as follows: All postoperative segments were merged into a single composite object as a stereolithography file, and the final 3D skull model was named "DESIGN." All mandibular segments, after completion of condylectomy and inferior mandibular border contouring, were registered to the original mandible and then combined to determine how much bone should be removed when condylectomy and mandibular border contouring were performed in view of the original mandible. The object of combination also was exported as a stereolithography file, named "MANDIBLE." This manipulation was accomplished using Geomagic (version 2012; 3D Systems, Rock Hill, SC) (Fig 4). DESIGN and MANDIBLE were imported into iPlan to be merged with the preoperative spiral CT images, and surgical navigation planning was performed.

SURGICAL PROCEDURE AND INTRAOPERATIVE NAVIGATION

The surgical procedure was conducted with the patient under general anesthesia, with nasotracheal intubation. Orthognathic surgery and condylectomy were simultaneously performed in each patient to correct the hypertrophic condyle, facial asymmetry, and malocclusion.

An extended buccal incision was made for SSO to perform coronoidectomy, after which the resected coronoid process was pushed upward to expose the condylar neck. Two holes were made astride the osteotomy line so that the coronoid process could be reset after condylectomy by means of stainless steel wire ligation. Under the guidance of the MANDIBLE file from the navigation system, condylectomy and inferior mandibular border contouring lines were marked using a fissure bur with the patient in centric occlusion before initiation of the orthognathic surgical procedure (Fig 5). A long titanium screw was fixed

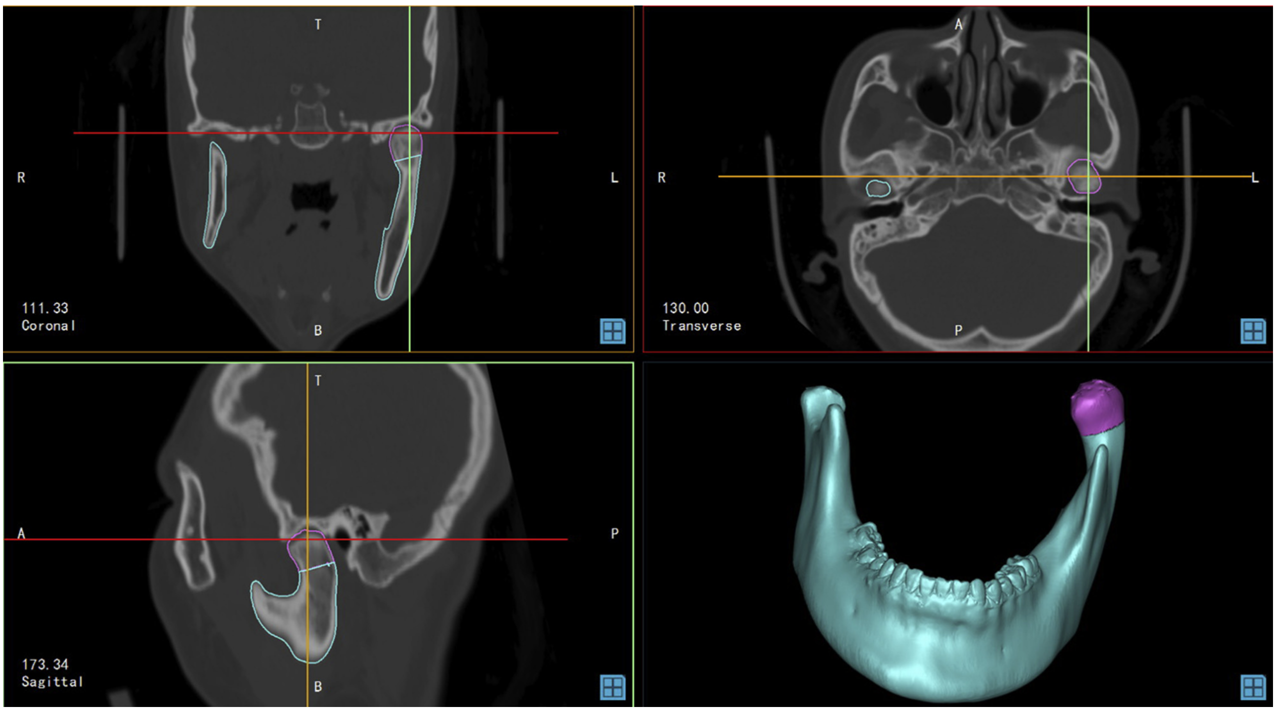

FIGURE 1. Design for condylectomy on affected side. A, anterior; B, bottom; L, left; P, posterior; R, right; T, top.

Han et al. Hemimandibular Hyperplasia Correction. J Oral Maxillofac Surg 2018.

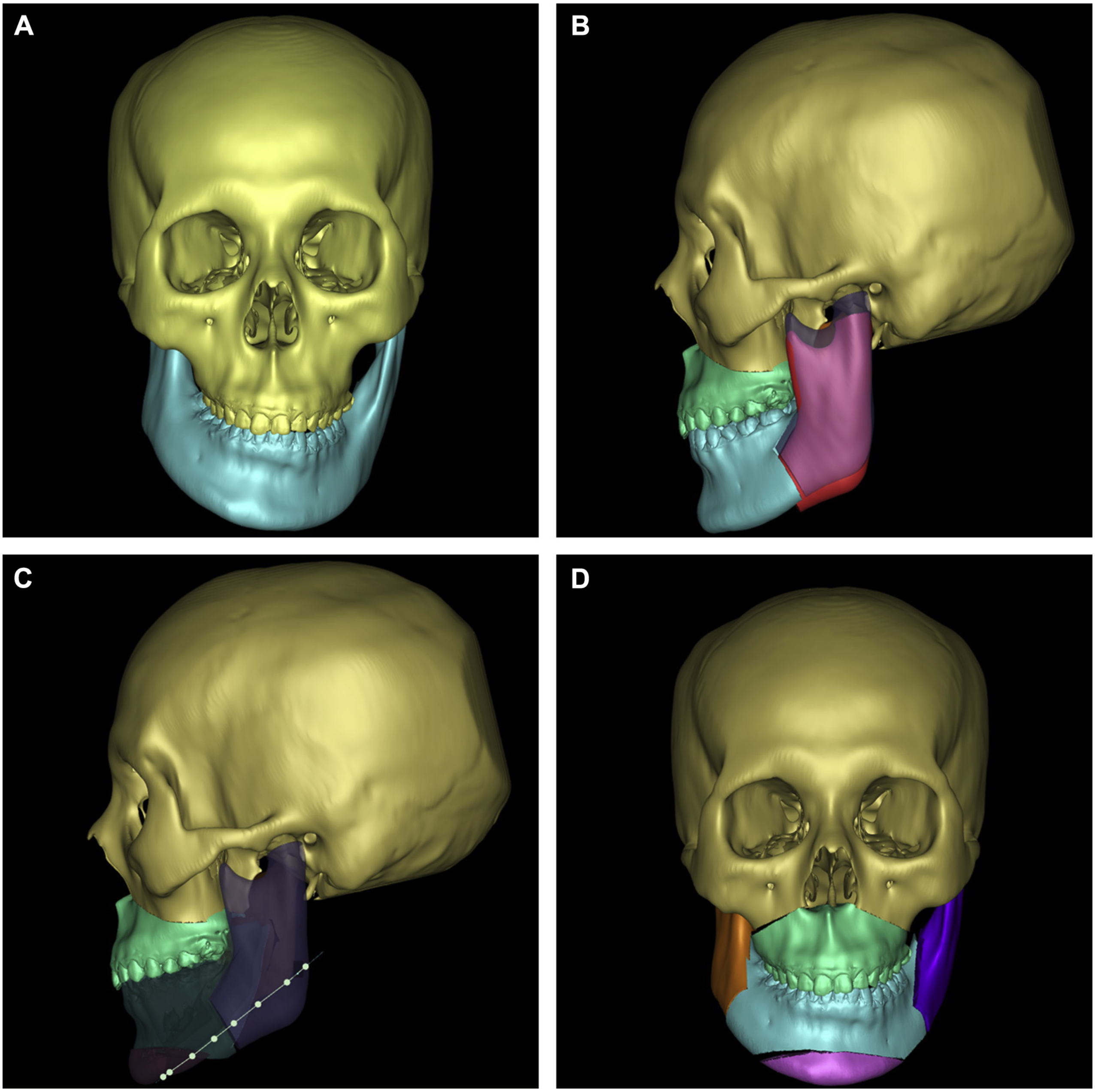

FIGURE 2. *A*, Original skull model. *B*, The proximal segment of the affected mandible was pushed upward into the glenoid fossa. *C*, Comparison of inferior border of mandible after condylectomy and bimaxillary orthognathic surgery and marking of range of inferior mandibular border contouring. *D*, Final 3-dimensional skull model after completion of mandibular border contouring.

Han et al. Hemimandibular Hyperplasia Correction. J Oral Maxillofac Surg 2018.

into the condyle to grasp it easily. Subsequently, a Le Fort I osteotomy was performed to correct the tilted occlusal plane, and the maxilla was repositioned and fixed under guidance of the intermediate occlusal splint. After disassembly of the intermaxillary fixation, BSSO and condylectomy were performed via an intraoral approach according to the marked lines. A specially designed retractor was placed between the condyle and its surrounding soft tissue to prevent any injury to the maxillary artery. The articular disc was maintained in its original position by blunt dissection after resection of the condylar head (Fig 6). Subsequently, a second intermaxillary fixation, determined by the terminal occlusal splint, was performed. Owing to the narrow field of vision available for condylectomy, removal of the resected condylar head, along with upward repositioning of the remaining ramus into the glenoid fossa for appropriate TMJ reconstruction, is challenging. In such cases, a Hopkins 30° endoscope (KARL STORZ SE & Co. Kg., Tuttlingen, Germany), 4 mm in diameter, through the intraoral incision helps provide better vision of the surgical field. Contouring

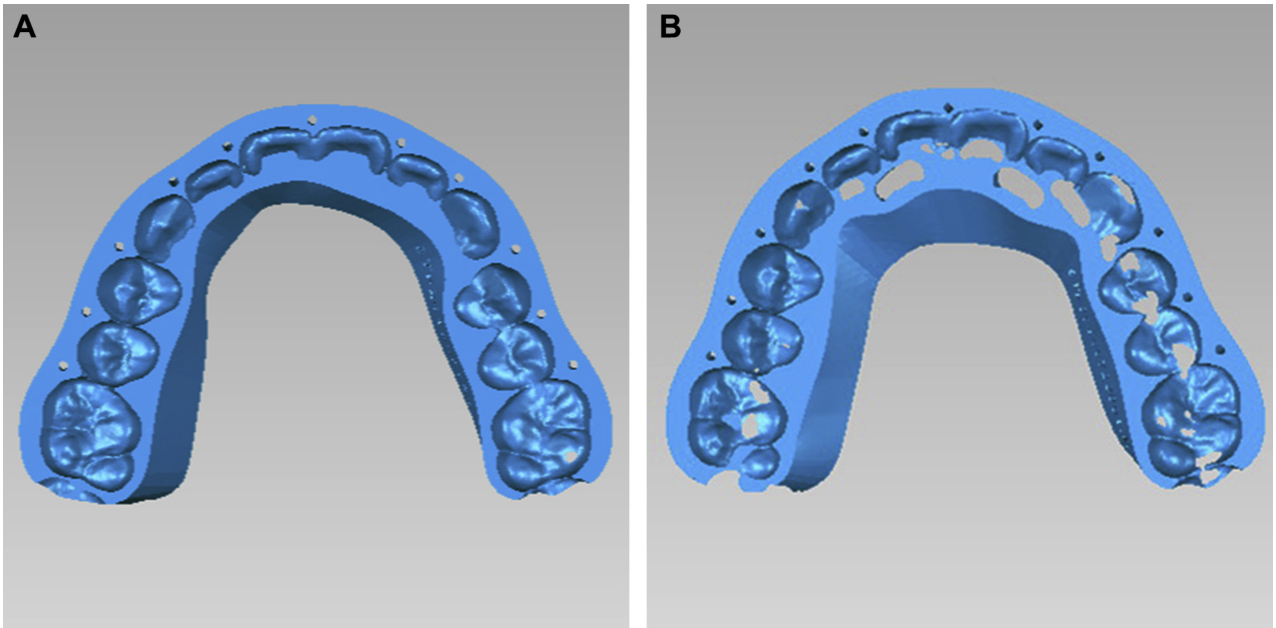

FIGURE 3. Occlusal splints produced using computer-aided manufacturing technology. *A*, Intermediate occlusal splints. *B*, Terminal occlusal splints.

Han et al. Hemimandibular Hyperplasia Correction. J Oral Maxillofac Surg 2018.

of the inferior mandibular border was performed by referring to the marked lines. Decortication of the inferior mandibular border was performed in certain cases, and the inferior alveolar nerves were carefully dissected and protected. Subsequently, the coronoid process was pulled down and reset by using stainless steel wires. After rigid fixation of the bilateral proximal and distal segments of the mandible with titanium plates, genioplasty was performed to further improve facial symmetry. After completion of orthognathic surgery with both the maxilla and mandible in the new position, the DESIGN file from the navigation system was used to check whether the bone stump of the condylar head was pushed upward into the exact

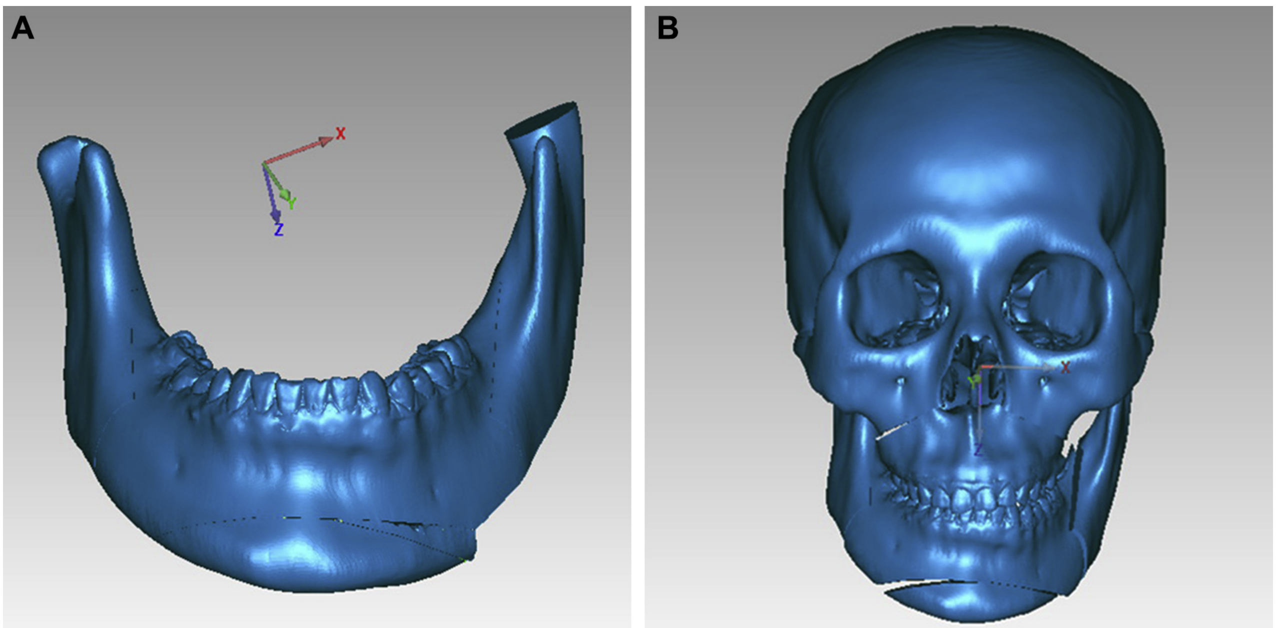

FIGURE 4. The DESIGN (*A*) and MANDIBLE (*B*) files were ready for surgical navigation.

Han et al. Hemimandibular Hyperplasia Correction. J Oral Maxillofac Surg 2018.

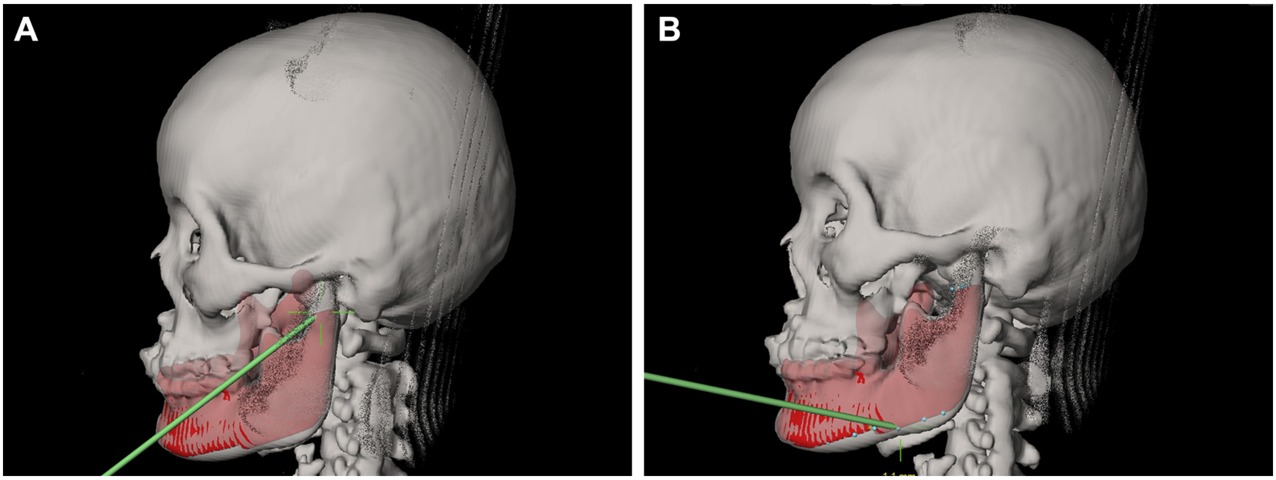

FIGURE 5. Surgical navigation during surgery. *A*, Marking of condylectomy line. *B*, Marking of osteotomy line for inferior mandibular border contouring.

Han et al. Hemimandibular Hyperplasia Correction. J Oral Maxillofac Surg 2018.

position and whether contouring of the mandibular border had been accomplished as presurgically planned (Fig 7). All resected condyles were subjected to histologic examination.

POSTOPERATIVE VALIDATION

Postoperative care included the antimicrobials cefoxitin sodium and metronidazole to avoid infection. Dexamethasone and vitamin C were applied to relieve swelling and facilitate healing; these also were routinely used during the perioperative period. Intermaxillary elastic traction was implemented 2 days after surgery to reach the final occlusal relationship guided by the terminal splint, and postoperative spiral CT images were recorded thereafter.

DESIGN was registered in the postoperative 3D skull model by using Geomagic. After manual and global registration, 3D comparisons were performed by considering DESIGN as the reference and the postoperative 3D skull model as the test object; color-coded mapping showed the 3D differences between these two. The affected and unaffected sides were divided into 4 regions: proximal segment of

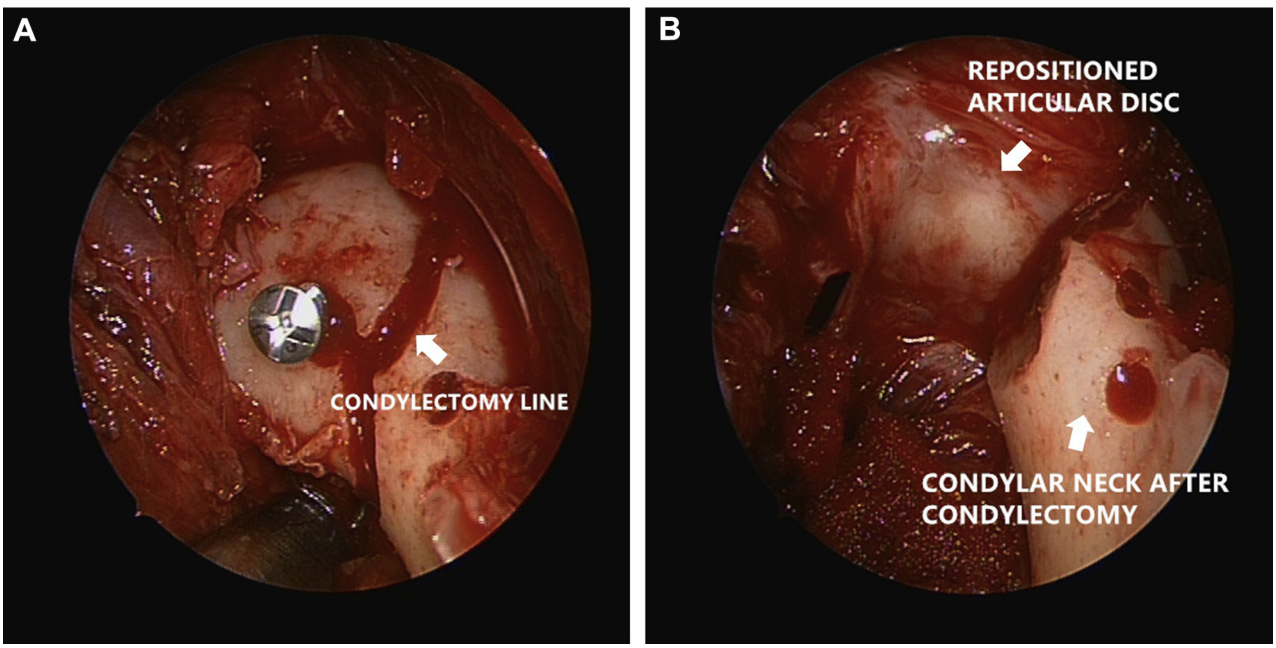

FIGURE 6. *A*, The condylectomy line was marked using a fissure bur with the patient in centric occlusion. *B*, The articular disc was maintained in its original position by blunt dissection after resection of the condylar head.

Han et al. Hemimandibular Hyperplasia Correction. J Oral Maxillofac Surg 2018.

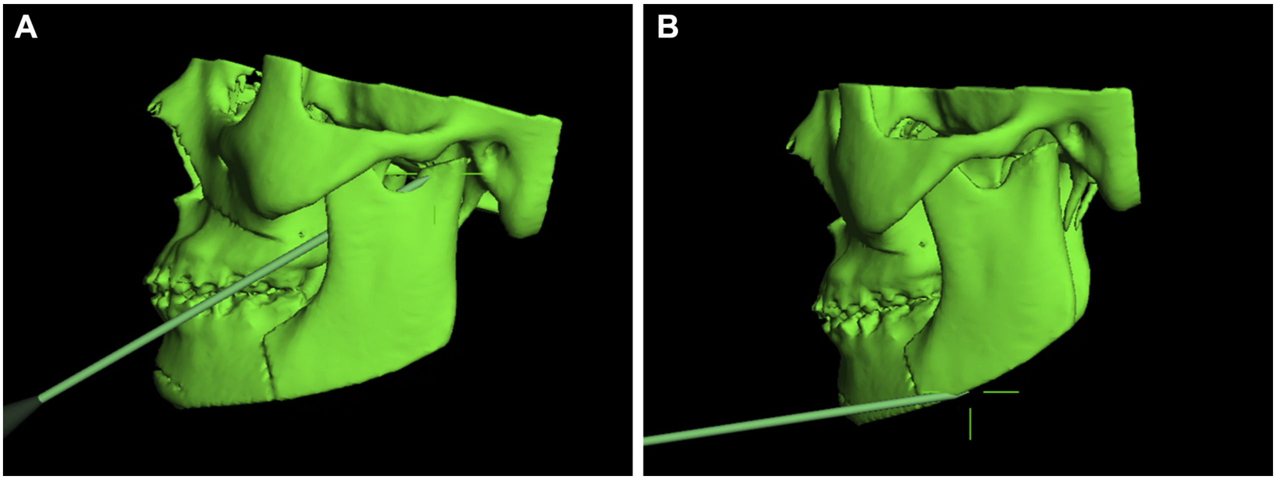

FIGURE 7. Validation of reconstructed condylar position (*A*) and postoperative inferior mandibular border (*B*) compared with presurgical design immediately after surgery.

Han et al. Hemimandibular Hyperplasia Correction. J Oral Maxillofac Surg 2018.

mandibular ramus (PSMR), proximal segment of mandibular body, distal segment of mandibular body, and maxillary segment. Mean differences in each region were separately calculated. To reduce calculation errors in 3D comparisons between DESIGN and postoperative 3D skull models of patients, the titanium plates as well as the teeth were excluded from the calculated region (Fig 8).

ASYMMETRY INDEX AND MEASUREMENT OF SYMMETRY

Preoperative and postoperative CT data were analyzed using ProPlan CMF software (version 1.3; Materialise Medical, Leuven, Belgium). The right porion and left porion, as well as the midpoint of the left orbitale and right orbitale, determined the Frankfort horizontal (FH) plane. The midsagittal reference (MSR) plane was perpendicular to the FH plane, passing the nasion and basion points.[23,24] The coronal plane was perpendicular to the FH and MSR planes, passing the nasion. We defined 7 pairs of bilateral landmarks (right and left) and 5 midline landmarks.[25] The distance from each point to the MSR, FH, and coronal planes was recorded as X, Y, and Z, respectively.

For evaluation of therapeutic efficacy, the asymmetry index (AI)[26] was used to show improvement in symmetry. The AI was calculated as follows:

$$AI = \sqrt{\Delta X^2 + \Delta Y^2 + \Delta Z^2}$$

where ΔX, ΔY, and ΔZ indicate the differences between the affected and unaffected sides.

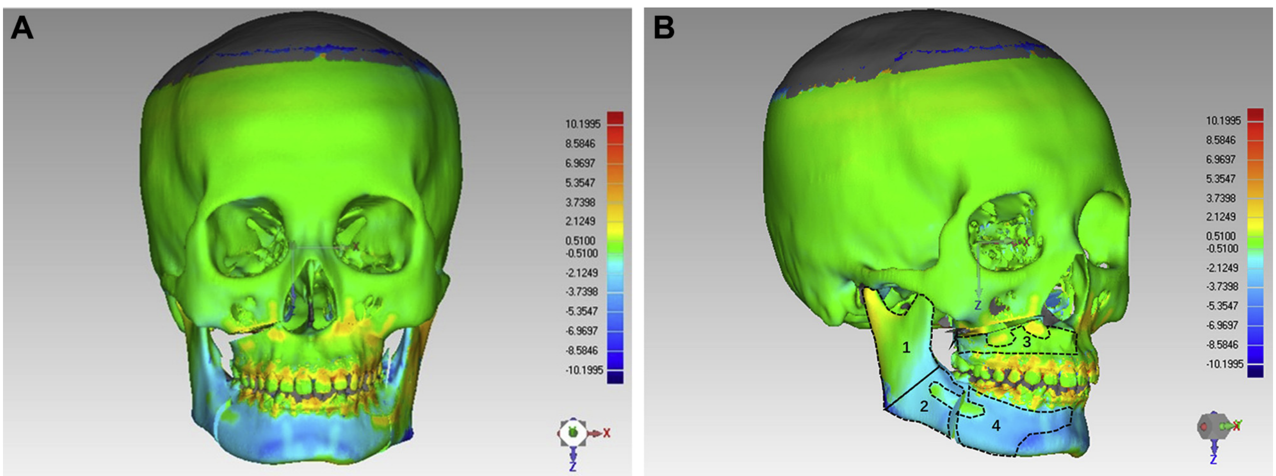

FIGURE 8. *A*, The metrology software produces a color map, showing the degree of deviation between test (postoperative 3-dimensional skull model) and reference (DESIGN) through different colors. *B*, Both the affected and unaffected sides were divided into 4 regions: *1)* proximal segment of mandibular ramus, *2)* proximal segment of mandibular body, *3)* maxillary segment, and *4)* distal segment of mandibular body.

Han et al. Hemimandibular Hyperplasia Correction. J Oral Maxillofac Surg 2018.

Landmarks are presented in Table 1 and Figure 9. Data were processed using IBM SPSS Statistics (version 20.0; IBM, Armonk, NY). The paired *t* test was used to determine any significant differences between preoperative-design skull model and postoperative real skull model measurements.

INTRAOBSERVER REPRODUCIBILITY

The defined bony landmarks (Table 2) were marked on the same patients 3 times at an interval of 2 weeks from the previous recording by the same researcher with more than 3 years of experience in orthognathic surgery. The same method was used for postoperative validation. The intraclass correlation coefficient (ICC) was calculated to validate intraobserver reproducibility.

Results

The mean age of enrolled patients (12 women and 2 men) was 26.7 years (range, 20 to 33 years). All 14 patients exhibited satisfactory clinical effects (Figs 10, 11) without complications, except 1 patient in whom mandibular vestibular incision infection developed 1 month after surgery, which was managed through wound irrigation. Facial symmetry improved as expected in all 14 patients. Operating room time was not absolutely decreased by using surgical virtual planning. The cost of using the CAD-CAM technique and surgical navigation system for each patient was approximately US $2,000. Because the costs of visual treatment objective, model surgery, and handcrafted occlusal splints were exempted, there was no marked increase in the economic burden for patients.

Table 1. DEFINITION OF LANDMARKS AND MEASUREMENTS

Landmark	Definition
Orbitale (O)	Most inferior point on inferior orbital rim
Porion (Po)	Most superior point of external acoustic meatus
Nasion (N)	Midpoint of frontonasal suture
Basion (Ba)	Most anterior point of foramen magnum
U6	Most inferior point of mesiobuccal cusp of each first upper molar
U3	Most inferior point of cusp of each upper canine
L6	Most superior point of mesiobuccal cusp of each first lower molar
L3	Most superior point of cusp of each lower canine
U1	Center of upper incisors
L1	Center of lower incisors
ANS	Tip of bony anterior nasal spine
Con	Lateral point of condyle
Gonion (Go)	Most inferior point on mandibular angle
Sig	Most inferior point of sigmoid notch
Pogonion (Pog)	Most anterior point of bony mandibular symphysis
Menton (Me)	Most inferior point of bony mandibular symphysis

Han et al. Hemimandibular Hyperplasia Correction. J Oral Maxillofac Surg 2018.

POSTOPERATIVE VALIDATION

The ICC of the bony landmark measurements performed on 3 occasions by an individual researcher was 0.956, which showed a high degree of correlation among these 3 sets of data. The mean distance of each segment measured in an individual patient was defined as M1. The mean value of each researcher's 3 measurements of M1 in each patient was defined as M2 (Fig 12).

Postoperative validation results showed that the expected outcomes of presurgical planning had been achieved more precisely on the unaffected side than on the affected side. The mandibular proximal segments on both sides exhibited a tendency for outward rotation compared with the presurgical planning model. On the other hand, the distal mandibular segments and both maxillary segments exhibited greater prominence on the affected side, which indicated that presurgical planning was not realized completely, thus necessitating overcorrection of the malformation.

MEASUREMENTS FOR EVALUATION OF FACIAL SYMMETRY

The X, Y, and Z measurements of each landmark were recorded, which constituted a group of data for 1 specific patient, and analyzed to evaluate the patient's facial symmetry. The ICC of these 3 times of data for the preoperative and postoperative 3D skull models, measured by the same researcher, was 0.987 and 0.997, respectively, which showed a high degree of correlation. AI values for each landmark were calculated from X, Y, and Z, and mean values of the 3 sets of data were obtained (Table 2). In addition, statistical analysis was performed to compare preoperative and postoperative facial symmetry.

The aforementioned findings showed that the tilted occlusal plane and deflective midline landmarks were corrected as expected after surgery. The tilted occlusal plane was less than 1 mm both at the most inferior point of the mesiobuccal cusp of the first upper molar and at the most inferior point of the cusp of the upper

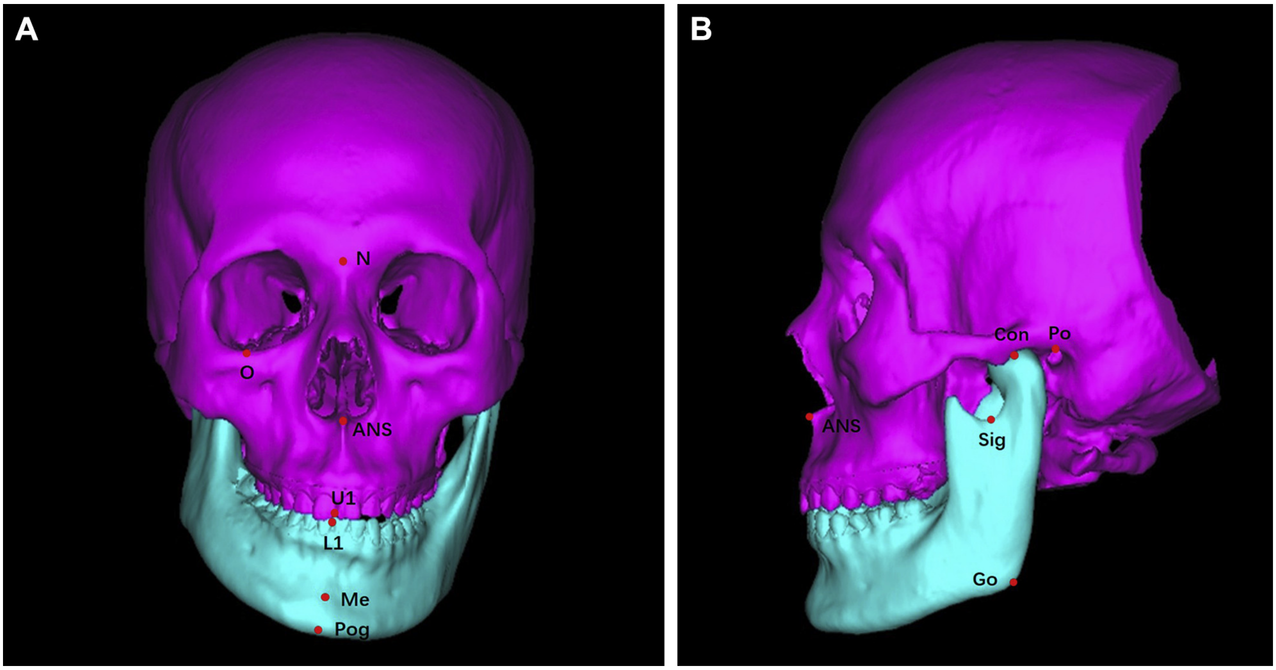

FIGURE 9. Landmarks in 3-dimensional skull model: frontal view (*A*) and left lateral view (*B*). ANS, tip of bony ANS; Con, lateral point of condyle; Go, gonion; L1, center of lower incisors; Me, menton; N, nasion; O, orbitale; Po, porion; Pog, pogonion; Sig, sigmoid notch; U1, center of upper incisors.

Han et al. Hemimandibular Hyperplasia Correction. J Oral Maxillofac Surg 2018.

canine after surgery. Although there were statistically significant differences between preoperative and postoperative gonion AI ($P < .01$) and sigmoid notch AI ($P < .01$) measurements, which indicated remarkable improvements in facial symmetry after surgery, a certain degree of bilateral mandibular ramus asymmetry still existed. These results showed that facial asymmetry could not be completely corrected even through extremely complex surgical procedures, but the degree of deviation was controlled under 2 mm, which cannot be easily perceived.

Because the AI was a positive value, it was difficult to determine whether a change, when it occurred, was a result of the correction or overcorrection of asymmetry; of note, ΔX, ΔY, and ΔZ could be helpful in identifying the origin of these changes. For most bilateral landmarks, the symmetry of X and Y had been improved as expected instead of Z, and overcorrection could hardly be noted in the results.

Discussion

HH is a type of condylar hyperplasia, according to the classification by Obwegeser and Makek[2] reported in 1986. The etiology of this disease remains unclear, and there are several opinions regarding the same. For example, the "local circulatory theory" claims that increased vascularization or a persistently high blood supply could lead to increased activity and growth.[27] Additional factors such as hormonal influences, heredity, infection, or trauma also have been considered.[9,28,29] HH has the following 4 specific characteristics: condylar hyperplasia, increased height of the mandibular body, tilted occlusal plane, and malocclusion. Orthognathic surgery with or without condylectomy is commonly considered for treatment of HH, which is indicated through abnormal imaging manifestations and bone scan findings. A previous study suggested that a relative percentage uptake of 55% or greater in the affected condyle indicates an active one and thus warrants condylectomy.[30]

In our study, ^{99m}Tc scintigraphy of both condyles was performed in all patients before surgery, and condylectomy was indicated when the uptake ratio between the affected and normal condyles was greater than 1.2, which was in accordance with the viewpoint of Pogrel.[30] Only 1 patient, with a ratio of 1.15, had undergone condylectomy because she complained about recent exacerbation of facial asymmetry and consented to undergo removal of the active condyle to prevent relapse of facial asymmetry.

Le Fort I osteotomy was performed to correct the compensatory maxillary growth on the affected side, which led to tilted occlusal planes. BSSO, as well as mandibular angle and body contouring, was performed to further correct the mandibular asymmetry. Because condylectomy had removed parts of the condylar head, determining the correct position of the bone stump in the glenoid fossa relative to the

Table 2. RESULTS OF PAIRED *T* TEST BETWEEN PREOPERATIVE AND POSTOPERATIVE MEASUREMENTS

Measurement (mm)	Preoperative, mean±SD	Postoperative, mean±SD	*t*	*P*
U6 AI	8.11 ± 3.15	3.25 ± 1.76	5.885	<.001
U6-ΔX	−3.42 ± 4.01	0.28 ± 3.24	−6.126	<.001
U6-ΔY	6.22 ± 2.78	0.19 ± 1.06	10.279	<.001
U6-ΔZ	0.33 ± 1.61	-0.31 ± 1.64	0.995	.338
U3 AI	6.44 ± 3.02	3.56 ± 2.26	3.339	.005
U3-ΔX	-3.62 ± 3.85	-0.48 ± 3.88	−4.553	.001
U3-ΔY	4.00 ± 2.24	0.10 ± 1.26	11.122	<.001
U3-ΔZ	0.67 ± 1.48	-0.07 ± 1.36	1.619	.129
L6 AI	11.64 ± 4.96	4.48 ± 2.49	4.866	<.001
L6-ΔX	−7.84 ± 6.36	−0.03 ± 4.43	−5.117	<.001
L6-ΔY	6.21 ± 3.40	0.36 ± 1.38	8.150	<.001
L6-ΔZ	−1.07 ± 3.09	−1.02 ± 2.40	−0.072	.943
L3 AI	11.72 ± 5.86	4.29 ± 2.49	4.435	.001
L3-ΔX	−9.18 ± 8.05	−0.93 ± 4.45	−4.309	.001
L3-ΔY	4.14 ± 2.16	0.73 ± 1.48	7.116	<.001
L3-ΔZ	−0.99 ± 1.57	−0.42 ± 1.52	−1.477	.163
Sig AI	12.93 ± 5.75	8.87 ± 5.27	2.591	.022
Sig-ΔX	−2.73 ± 6.64	2.26 ± 7.48	−2.654	.020
Sig-ΔY	9.70 ± 6.91	−0.22 ± 4.68	7.145	<.001
Sig-ΔZ	0.50 ± 3.45	1.32 ± 5.21	−0.685	.505
Con AI	6.72 ± 3.39	7.62 ± 3.44	−0.961	.354
Con-ΔX	1.33 ± 3.45	0.55 ± 4.55	0.761	.460
Con-ΔY	3.48 ± 3.41	1.37 ± 4.67	1.661	.121
Con-ΔZ	−0.60 ± 4.62	2.16 ± 4.93	−2.376	.034
Go AI	23.19 ± 9.69	10.40 ± 4.84	4.711	<.001
Go-ΔX	−15.85 ± 8.92	−3.49 ± 6.23	−6.654	<.001
Go-ΔY	14.80 ± 8.21	1.75 ± 7.64	10.825	<.001
Go-ΔZ	0.76 ± 4.39	1.06 ± 5.00	−0.210	.837
ANS-X	1.54 ± 1.07	1.50 ± 1.27	0.075	.941
11M-X	2.72 ± 1.93	1.49 ± 1.16	1.984	.069
31M-X	5.34 ± 2.93	1.75 ± 1.29	4.207	.001
Pog-X	10.90 ± 4.13	1.81 ± 1.03	7.832	<.001
Me-X	13.37 ± 5.74	1.77 ± 1.18	7.219	<.001

Abbreviations: 11M, the midpoint of central incisor of maxilla; 31M, the midpoint of central incisor of mandible; AI, asymmetry index; ANS, tip of bony anterior nasal spine; Con, lateral point of condyle; Go, gonion; L6, most superior point of mesiobuccal cusp of first lower molar; L3, most superior point of cusp of lower canine; Me, menton; Pog, pogonion; Sig, sigmoid notch; SD, standard deviation; U6, most inferior point of mesiobuccal cusp of first upper molar; U3, most inferior point of cusp of upper canine.

Han et al. Hemimandibular Hyperplasia Correction. J Oral Maxillofac Surg 2018.

preoperative design finalized for TMJ reconstruction was challenging. To resolve this, the MANDIBLE and DESIGN files exported into the navigation system played important roles in improving surgical precision, which was a novel concept used in comparison with the previous study. On postoperative validation, the median of M2 on both sides was a positive value. Although we excluded the teeth and titanium plates while performing measurements, bone grafting may still produce errors. The values of the affected side were larger than those of the unaffected side, which indicated a possibility of mild deformity and that the design could not be completely realized. Thus, overcorrection may be necessary. However, the appropriate amount of overcorrection remains unclear and warrants further research. Apart from PSMR and the proximal segment of the mandibular body, the maxillary segment and the distal segment of the mandibular body showed a smaller degree of variation between the design and postoperative real skull model because the occlusal splints used during the surgical procedure can help ensure positioning to be as precise as the preoperative design.

After SSO, both ends of the proximal mandibular segment were free before fixation, particularly on the affected side. Usually, it is difficult for surgeons to ensure appropriate positioning of the condylar stump under poor vision during surgery. Although

FIGURE 10. Clinical images of patient preoperatively (*A-D*), 3 months after surgery (*E-H*), and 1 year after surgery (*I-L*). **(Fig 10 continued on next page.)**

Han et al. Hemimandibular Hyperplasia Correction. J Oral Maxillofac Surg 2018.

FIGURE 10 (cont'd). **(Fig 10 continued on next page.)**

Han et al. Hemimandibular Hyperplasia Correction. J Oral Maxillofac Surg 2018.

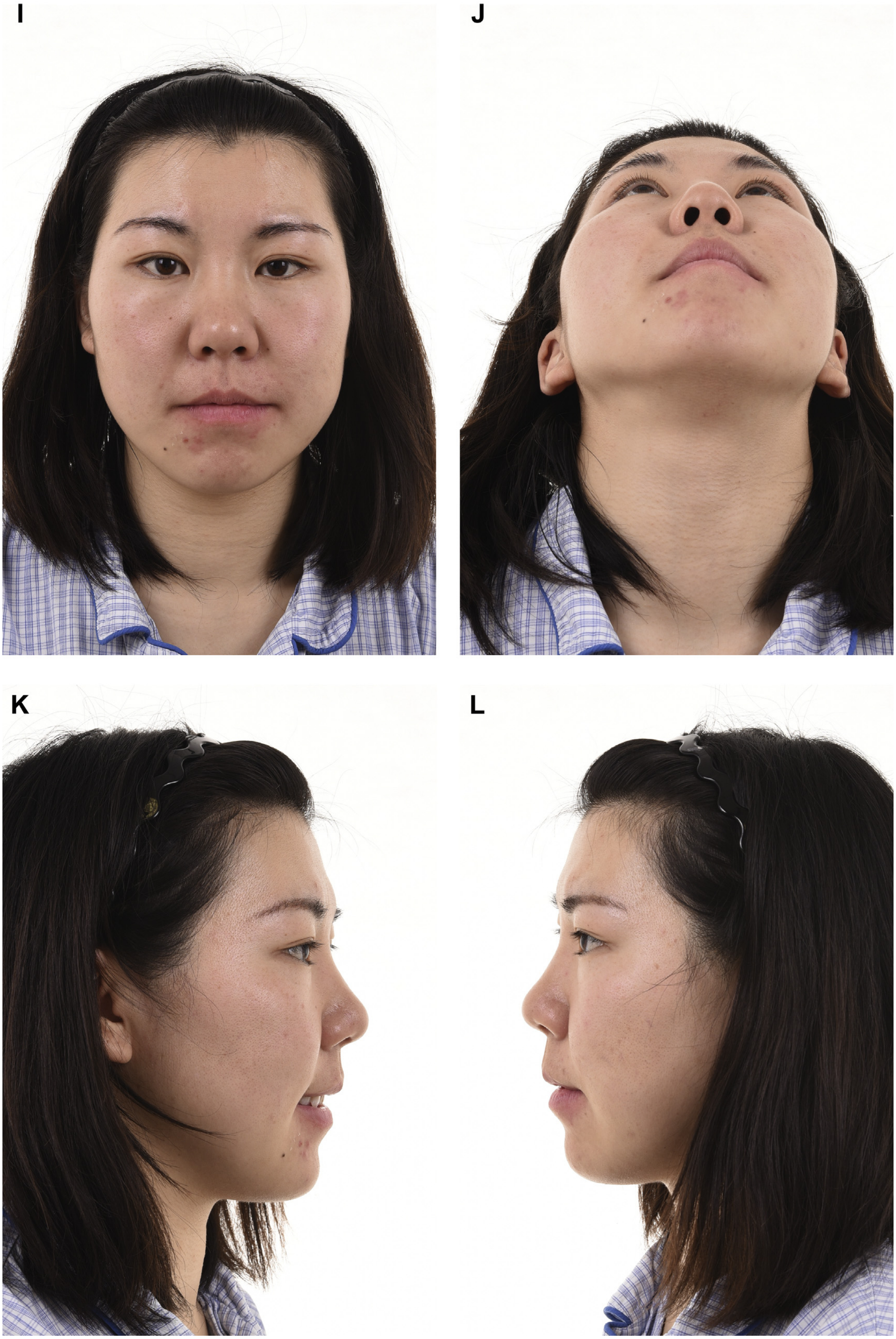

FIGURE 10 (cont'd).

Han et al. Hemimandibular Hyperplasia Correction. J Oral Maxillofac Surg 2018.

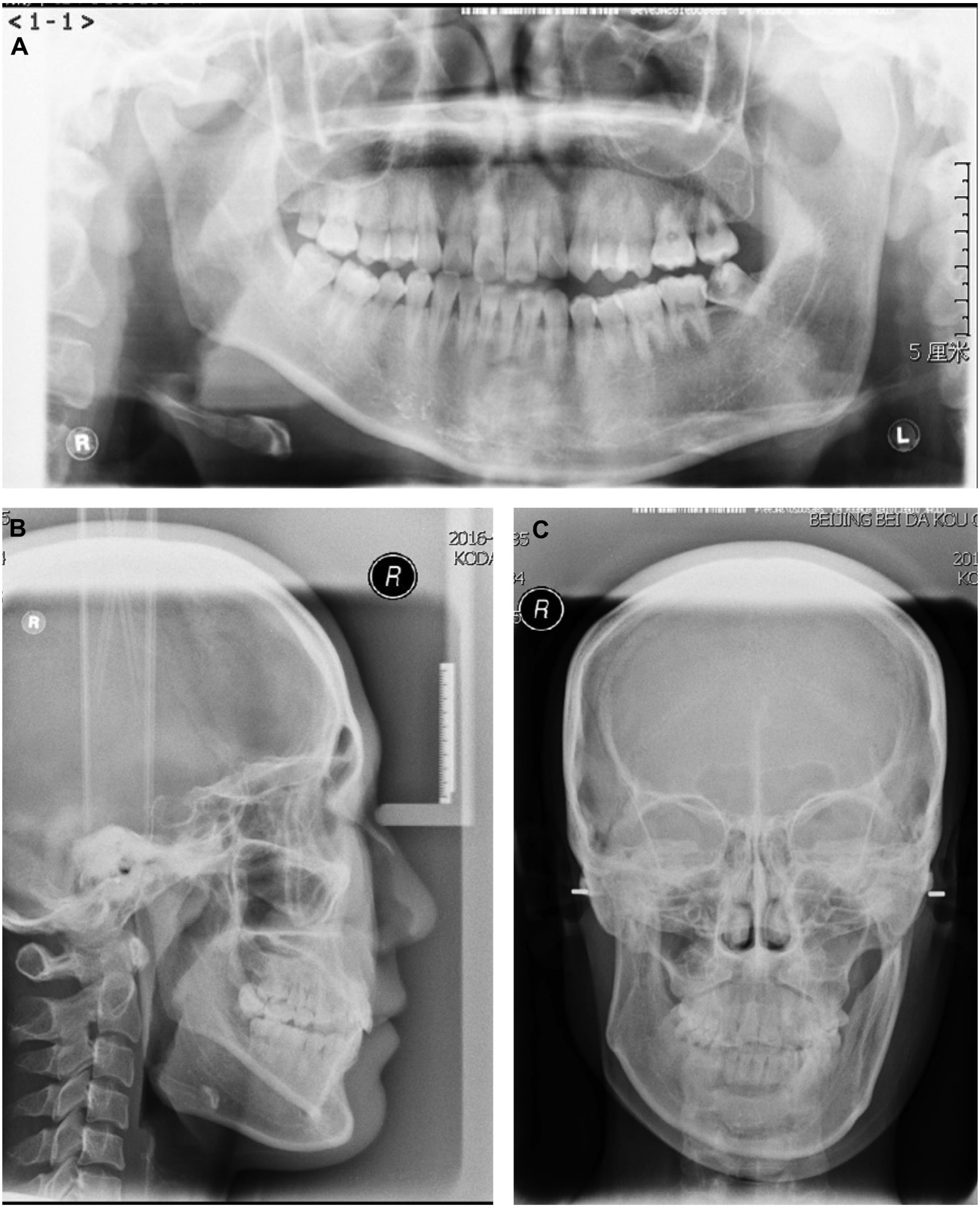

FIGURE 11. *A-C*, Preoperative radiographs. *D-F*, Postoperative radiographs. *G-I*, Radiographs 1 year after surgery. L, left; R, right. **(Fig 11 continued on next page.)**

Han et al. Hemimandibular Hyperplasia Correction. J Oral Maxillofac Surg 2018.

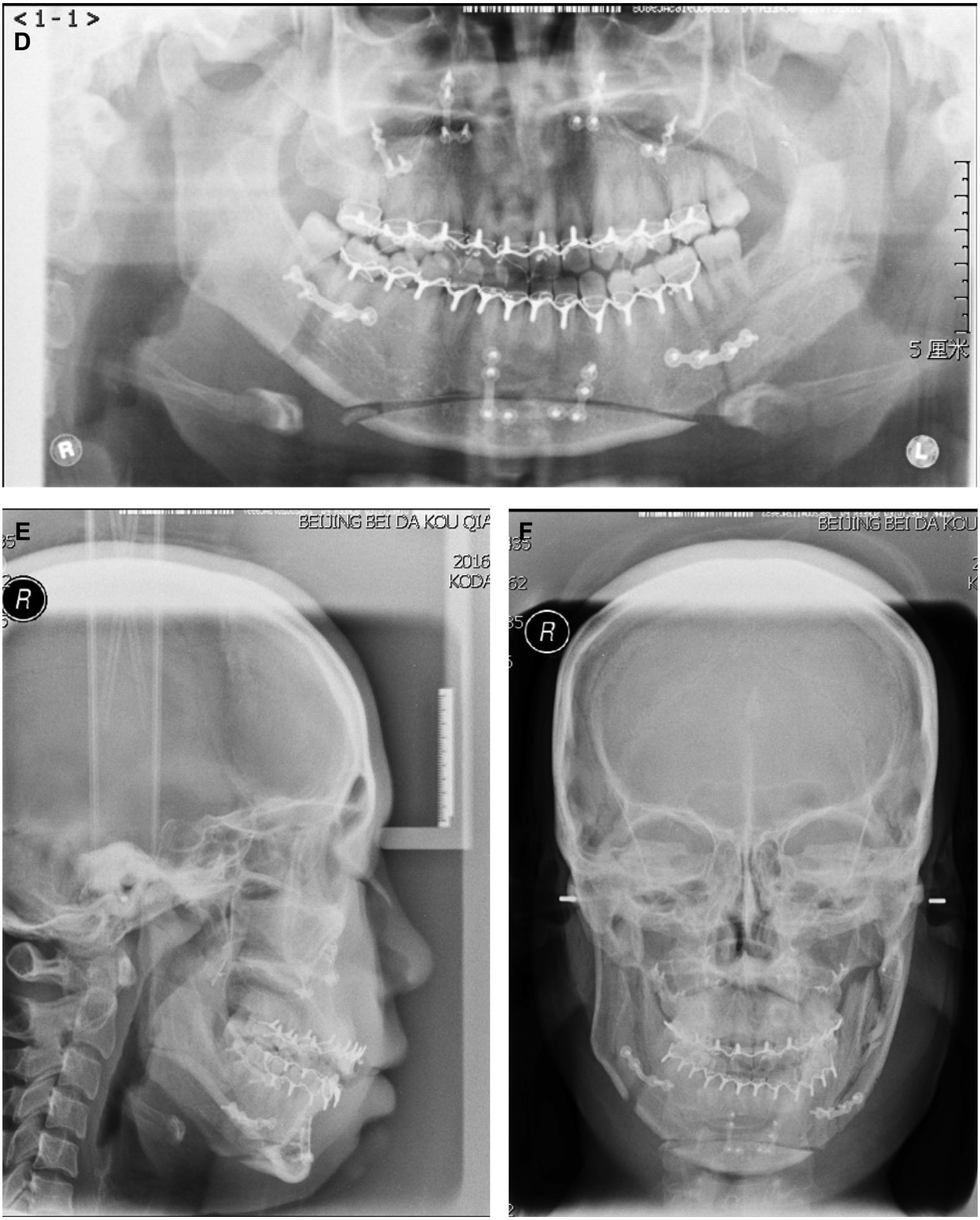

FIGURE 11 (cont'd). **(Fig 11 continued on next page.)**

Han et al. Hemimandibular Hyperplasia Correction. J Oral Maxillofac Surg 2018.

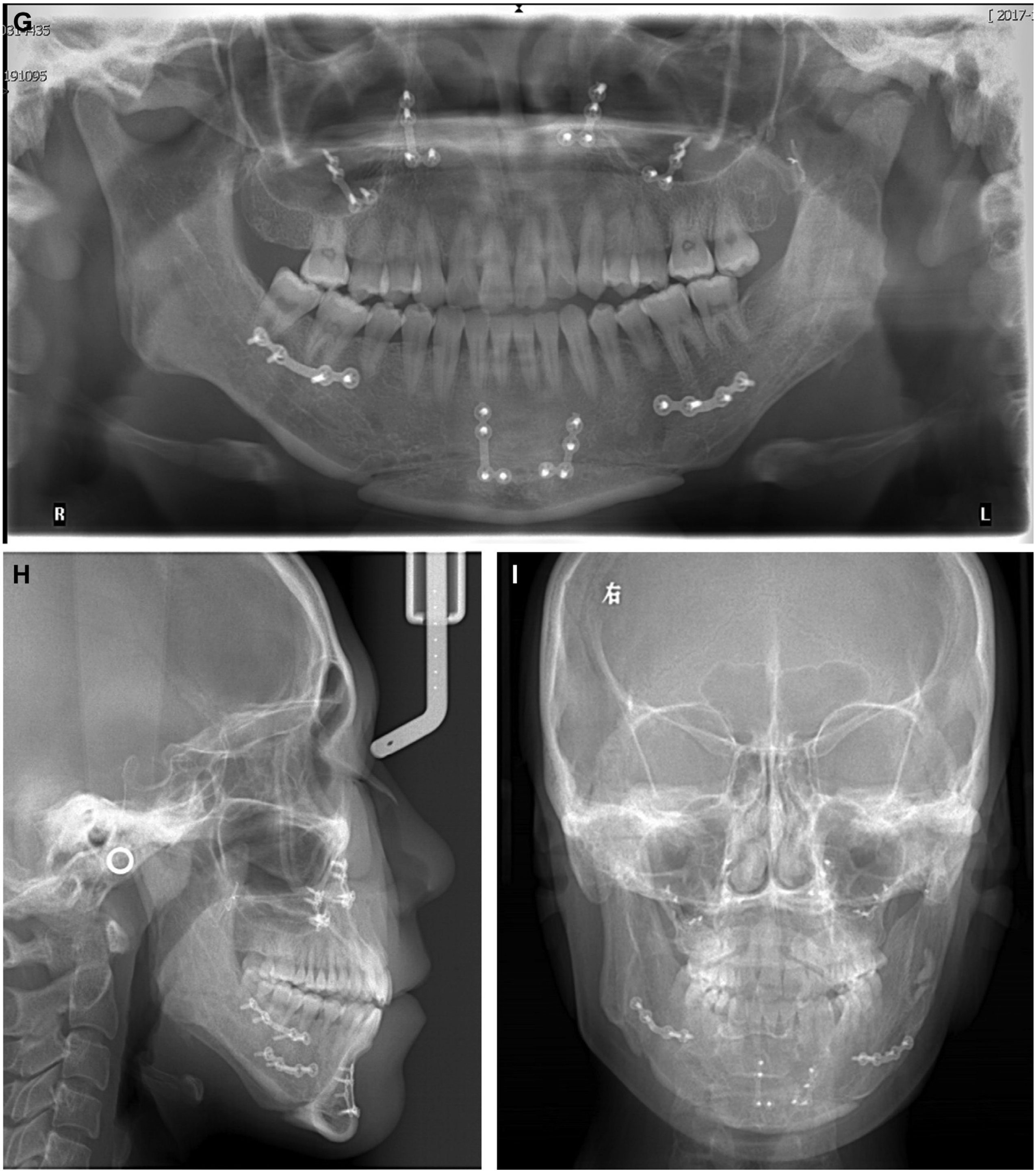

FIGURE 11 (cont'd).

Han et al. Hemimandibular Hyperplasia Correction. J Oral Maxillofac Surg 2018.

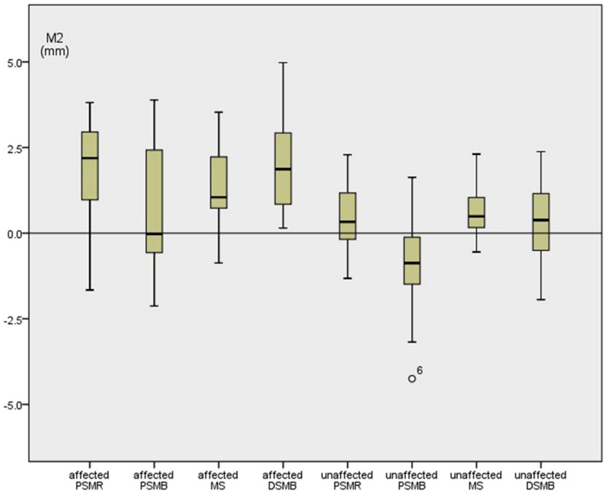

FIGURE 12. Box plot of M2 of proximal segment of mandibular ramus (PSMR), proximal segment of mandibular body (PSMB), maxillary segment (MS), and distal segment of mandibular body (DSMB) on affected and unaffected sides in 14 patients. M2, the mean value of each researcher's 3 measurements of M1 in each patient.

Han et al. Hemimandibular Hyperplasia Correction. J Oral Maxillofac Surg 2018.

virtual navigation can provide assistance during surgery and can validate results immediately after surgery, it is still difficult to avoid all errors during condylar positioning. In our study, although the PSMR of the affected side seemed to be going outward, no statistical differences were noted between the preoperative and postoperative AI as well as ΔX of the lateral point of the condyle. A possible reason is that the hyperplastic condyle was more outward in the fossa than the normal condyle before surgery; hence, the difference between preoperative and postoperative condylar position on the affected side was small. Moreover, insertion of an additional bicortical miniscrew in the ramus area may be an effective measure to alleviate the rotation of the PSMR on the affected side because it can bring the proximal and distal segments much closer and stabilize them further. However, the feasibility of this step warrants further research and validation.

When symmetry was assessed, landmarks in the distal segments of the maxilla and mandible showed better symmetry than those in the respective proximal segments. This could be because occlusal splints ensured positioning of the maxillary proximal segments whereas positioning of the mandibular proximal segments relied on the surgeon's experience. Hence, it was difficult to determine the exact degree of mandibular contouring required to achieve bilateral symmetry. Although presurgical virtual planning and surgical navigation were used to assist in positioning of the mandibular distal segments and contouring, landmarks at the mandibular distal segments such as the gonion still showed greater variability. Additional studies are warranted to improve such correction results.

Data on ΔX, ΔY, and ΔZ indicated that facial asymmetry was primarily reflected in ΔX and ΔY before surgery. Thus, ΔZ of most landmarks showed only slight postoperative changes, if at all, and contributed most toward postoperative asymmetry, which was consistent with our postoperative validation results. This was because facial asymmetry is primarily manifested at X and Y rather than at Z.

On the basis of the results of our study, we can conclude that orthognathic surgery with simultaneous condylectomy under digital assistance is a realistic and precise treatment technique. The precision of the TMJ reconstruction by positioning of the condylar stump into the glenoid fossa on the affected side can be validated during surgery instead of through postoperative spiral CT performed several days later, which can avoid a probable second surgical procedure or reoperation to manage condylar malposition. However, movement of each segment cannot be accurately controlled, and additional studies are needed to focus on how to improve precision while implementing presurgical virtual planning. Foundation items: Capital Characteristic Clinical Research Projects (Z161100000516114)

References

1. Adams R: Case history of Mary Keefe, *in* Medical Section of the British Association. Bristol Meeting, 1836
2. Obwegeser HL, Makek MS: Hemimandibular hyperplasia—Hemimandibular elongation. J Maxillofac Surg 14:183, 1986
3. Chen Y-R, Bendor-Samuel RL, Huang C-S: Hemimandibular hyperplasia. Plast Reconstr Surg 97:730, 1996
4. Pelo S, Correra P, Gasparini G, et al: Three-dimensional analysis and treatment planning of hemimandibular hyperplasia. J Craniofac Surg 22:2227, 2011
5. Matteson SR, Proffit WR, Terry BC, et al: Bone scanning with 99mtechnetium phosphate to assess condylar hyperplasia. Report of two cases. Oral Surg Oral Med Oral Pathol 60:356, 1985
6. Wolford LM, Movahed R, Perez DE: A classification system for conditions causing condylar hyperplasia. J Oral Maxillofac Surg 72:567, 2014
7. Wolford LM: Clinical indications for simultaneous TMJ and orthognathic surgery. Cranio 25:273, 2007
8. Wolford LM, Movahed R, Dhameja A, Allen WR: Low condylectomy and orthognathic surgery to treat mandibular condylar osteochondroma: A retrospective review of 37 cases. J Oral Maxillofac Surg 72:1704, 2014
9. Lippold C, Kruse-Losler B, Danesh G, et al: Treatment of hemimandibular hyperplasia: The biological basis of condylectomy. Br J Oral Maxillofac Surg 45:353, 2007
10. Angiero F, Farronato G, Benedicenti S, et al: Mandibular condylar hyperplasia: Clinical, histopathological, and treatment considerations. Cranio 27:24, 2009
11. Wolford LM, Morales-Ryan CA, Garcia-Morales P, Perez D: Surgical management of mandibular condylar hyperplasia type 1. Proc (Bayl Univ Med Cent) 22:321, 2009
12. Hernandez-Alfaro F, Mendez-Manjon I, Valls-Ontanon A, Guijarro-Martinez R: Minimally invasive intraoral condylectomy: Proof of concept report. Int J Oral Maxillofac Surg 45:1108, 2016

13. Kumar VV: Large osteochondroma of the mandibular condyle treated by condylectomy using a transzygomatic approach. Int J Oral Maxillofac Surg 39:188, 2010
14. Vezeau PJ, Fridrich KL, Vincent SD: Osteochondroma of the mandibular condyle: Literature review and report of two atypical cases. J Oral Maxillofac Surg 53:954, 1995
15. Kurita K, Ogi N, Echiverre NV, Yoshida K: Osteochondroma of the mandibular condyle. A case report. Int J Oral Maxillofac Surg 28:380, 1999
16. Schoen R, Herklotz I, Metzger MC, et al: Endoscopic approach to removal of an osteochondroma of the mandibular condyle. J Oral Maxillofac Surg 69:1657, 2011
17. Wang XX, Li ZL, Yi B, et al: [Clinical application of condylectomy via intraoral approach under computer assisted surgical navigation]. Zhonghua Kou Qiang Yi Xue Za Zhi 48:350, 2013 (in Chinese)
18. Zhou H, Liao C, Hu J, Fei W: Comparison of the clinical effects of treatment of osteochondroma by two types of vertical ramus osteotomy. Br J Oral Maxillofac Surg 56:19, 2018
19. Yu H, Jiao F, Li B, et al: Endoscope-assisted conservative condylectomy combined with orthognathic surgery in the treatment of mandibular condylar osteochondroma. J Craniofac Surg 25: 1379, 2014
20. Wang XX, Li ZL, Yi B, et al: [Preliminary study of condylectomy via intraoral approach]. Zhonghua Kou Qiang Yi Xue Za Zhi 47: 305, 2012 (in Chinese)
21. Tian K, Xue Z, Liu X, et al: Recording and transferring head positions to the virtual head using a multicamera system and laser level. J Oral Maxillofac Surg 73:2039.e1, 2015
22. Tian K, Li Q, Wang X, et al: Reproducibility of natural head position in normal Chinese people. Am J Orthod Dentofacial Orthop 148:503, 2015
23. Choi JW, Jung SY, Kim HJ, Lee SH: Positional symmetry of porion and external auditory meatus in facial asymmetry. Maxillofac Plast Reconstr Surg 37:33, 2015
24. Lonic D, Sundoro A, Lin HH, et al: Selection of a horizontal reference plane in 3D evaluation: Identifying facial asymmetry and occlusal cant in orthognathic surgery planning. Sci Rep 7:2157, 2017
25. Kwon TG, Park HS, Ryoo HM, Lee SH: A comparison of craniofacial morphology in patients with and without facial asymmetry—A three-dimensional analysis with computed tomography. Int J Oral Maxillofac Surg 35:43, 2006
26. Maeda M, Katsumata A, Ariji Y, et al: 3D-CT evaluation of facial asymmetry in patients with maxillofacial deformities. Oral Surg Oral Med Oral Pathol Oral Radiol Endod 102:382, 2006
27. Oberg T, Fajers CM, Lysell G, Friberg U: Unilateral hyperplasia of the mandibular condylar process. A histological, microradiographic, and autoradiographic examination of one case. Acta Odontol Scand 20:485, 1962
28. Gray RJ, Sloan P, Quayle AA, Carter DH: Histopathological and scintigraphic features of condylar hyperplasia. Int J Oral Maxillofac Surg 19:65, 1990
29. Gottlieb O: [Unilateral mandibular hyperplasia]. Tandlaegebladet 56:211, 1952 (in Danish)
30. Pogrel MA: Quantitative assessment of isotope activity in the temporomandibular joint regions as a means of assessing unilateral condylar hypertrophy. Oral Surg Oral Med Oral Pathol 60: 15, 1985